ENRICHMENT OF SURFACE MORPHOLOGY AND MECHANICAL BEHAVIOUR OF MAGNESIUM ALLOY COMPOSITE MADE WITH HYBRID REINFORCEMENTS VIA VACUUM-AIDED STIR CAST PROCESS

Ramesh Dnyando Sul
Department of Chemistry, D Y Patil College of Engineering, Akurdi, Pune, Maharashtra 411044, India

Nitin Kundlik
Department of Robotics and Automation, D Y Patil College of Engineering, Akurdi, Pune, Maharashtra 411044, India

Aman Sharma
Department of Mechanical Engineering, Institute of Engineering and Technology, GLA University, Mathura, Uttar Pradesh 281406, India

V. Muthuraman
Department of Mechanical Engineering, Vels Institute of Science, Technology and Advanced Studies, Pallavaram, Chennai, Tamil Nadu 600117, India

Sendil Kumar
Department of Education, Senthil College of Education, Puducherry 605110, India

Nagabhooshanam Nagarajan
Department of Mechanical Engineering, Aditya University, Surampalem, Andhra Pradesh 533437, India
Department of Mechanical Engineering, Institute of Engineering and Technology, GLA University, Mathura, Uttar Pradesh 281406, India

BEVL Naidu
Department of Management Studies, Aditya Degree & PG College(A), Kakinada, Andhra Pradesh 533003, India

Ramya Maranan
Division of Research and Development, Lovely Professional University, Jalandhar - Delhi G.T. Road, Phagwara, Punjab 144411, India

T. Thirugnanasambandham
Department of Mechanical Engineering, Saveetha School of Engineering, Saveetha Institute of Medical and Technical Sciences, SIMATS, Chennai, Tamil Nadu 602105, India

https://doi.org/10.1007/s40962-025-01807-0

Abstract

A hybrid magnesium matrix composite reinforced with aluminum, zinc, and multiple particulates was developed through liquid stir casting to enhance tribo-mechanical performance for potential applications in automotive housings and structural frames. However, conventional stir casting often results in reinforcement agglomeration, porosity due to gas entrapment and oxide formation, and non-uniform particle distribution, which limit composite performance. This study aims to enhance the functional characteristics of an AZ91 magnesium alloy by incorporating nanoscale silicon carbide (SiC, 50 nm) and graphene (0.5 µm in length, 30 nm thick) as reinforcements. A vacuum-assisted stir casting process was employed, with a constant stirring rate and argon shielding to minimize oxidation and promote uniform dispersion of the material.

Received: 15 June 2025 / Accepted: 06 November 2025
Published online: 16 November 2025

The synthesized AZ91-based composite contained 0.5 wt.% graphene and 2–6 wt.% nano-SiC. The effects of vacuum-assisted casting and hybrid reinforcement on the microstructure (as observed via scanning electron microscopy), mechanical properties (including tensile strength, elongation, Vickers hardness, and energy absorption), and density/porosity were evaluated and compared with those of the unreinforced AZ91 alloy. Microstructural analysis revealed improved dispersion and interfacial bonding between SiC and graphene within the matrix under vacuum. The AZ91–0.5 wt.% graphene 6 wt.% SiC nanocomposite exhibited superior properties, including a tensile strength of 303 MPa, hardness of 105 HV, energy absorption of 13.7 J, and a reduced porosity level of 0.7%. These enhancements demonstrate the potential of the developed hybrid nanocomposite for applications like structural components in the automotive sector.

Keywords: *AZ91 alloy, hybrid reinforcements, microstructure, porosity, stir cast*

Introduction

With key benefits including lightweight properties, increased yield and tensile strength, higher energy absorption, and improved tribological behaviour, magnesium alloy composites are utilized for automotive housing, structural, and aerospace cabin parts.[1,2] Conventional stir casting was employed for magnesium alloy composites due to its ease of processing, economic viability, suitability for complex design preparation, and scalability.[3] However, oxide and entrapped gas formation led to higher porosity, which reduced the composite's functional behaviour.[4] It was overcome by an argon shield gas approach used throughout the process.[5] Moreover, a magnesium alloy with an aluminum–zinc composition, embedded with nanoceramic particles via liquid-phase stir casting at a constant stir speed (400 rpm) in a semi-solid state, exhibited uniform reinforcement dispersion and superior functional behaviour.[6]

Venkatesh et al. [7] investigated the functional characteristics of AZ91 series alloy hybrid composites composed of 3% BN (boron nitride) and varying percentages of TiO_2 (titanium dioxide) nanoparticles, using a two-step stir casting process. Semi-solid stir-processed AZ91 series alloy hybrid nanocomposites with 3% and 5% BN/TiO_2 combinations exhibit improved microstructural behaviour, accompanied by enhanced tensile, impact, and hardness properties. The titanium (Ti)/silicon carbide (SiC) particles embedded in the AZ91 composite were produced via the stir casting route. The applied argon shield gas and uniform blending action resulted in a homogeneous Ti/SiC dispersion, leading to superior compression and tensile strength behaviour, exceeding that of monolithic AZ91.[8] The AZ91 hybrid composite was developed and evaluated for its functional and microstructural behaviour. The combined action of SiC and fly ash resulted in a higher tensile stress. More than 3% of fly ash leads to agglomeration and reduces the tribo-mechanical behaviour of composites.[9] The ZE41 series of magnesium alloy composites was developed using graphene nanoparticles via the stir cast technique, and its functional characteristics were investigated. The composite contained 12% reinforcement, which exhibited the greatest compression strength behaviour, and a stir speed of 400 rpm with a 15-minute blending time, providing homogeneous reinforcement distribution.[10] Kumar and Sozhamannan [11] synthesized and investigated the hardness, energy absorption, and tensile stress behaviour of a magnesium alloy composite prepared with 0.5–1.5% graphene particles via the stir cast technique. The composite, composed of 0.5% graphene, showed higher energy absorption, better hardness, and enhanced tensile stress behaviour than the monolithic AZ91D. Using the ultrasonic-assisted stir cast technique, an AZ91/Al_2O_3 (alumina)/TiB_2 (titanium diboride) hybrid composite was developed, and its functional properties were investigated. The application of 400 rpm and 20 kW results in uniform dispersion of Al_2O_3/TiB_2 particles, leading to increased hardness, energy absorption, and tensile strength properties, exceeding those of AZ91.[12] The vacuum-aided stir cast technology adopted for AZ80 hybrid composite fabrication and the composite processed with $1x10^5$ pa vacuum pressure leads to improved composite quality and reduced porosity, with hiked bonding strength between the matrix and SiC/basalt fiber (BF), resulting in superior hardness, better energy absorption behaviour, hiked tensile strength, and improved wear resistance property.[13] The Al-Zn-Mg alloy composite was fabricated using nano-silicon nitride (Si_3N_4) and boron nitride (BN) via a vacuum-aided stir casting method. It analyzed its microstructural and mechanical properties, including hardness, tensile, compression, and impact strengths. The composite of Al-Zn-Mg with 6% Si_3N_4 and 9% BN exhibited superior hardness, impact, compression, and tensile stress behaviour.[14] Moreover, the advanced stir cast process, with optimal process parameters and a suitable reinforcement content, influenced the quality and functional properties of the composite.[15] The vacuum-assisted stir casting technique offers a trade-off between mass production and is suitable for fabricating magnesium hybrid composites.[16,17] Kaliyannan et al. [18] developed and investigated the microstructural and functional characteristics of an LM25 alloy composite containing graphite and breadfruit seed husk ash, produced by squeeze casting. The contribution of husk ash could reduce the composite's density and, when

combined with graphite particles, provide high stress concentration behaviour with superior tensile and corrosion resistance compared to the monolithic alloy. However, nano-sized silicon carbide particles could provide better interfacial behaviour and be used in lightweight polymer-based composite applications.[19,20] Not only does a polymer matrix, which plays a crucial role in metal matrix composites, influence the interfacial action between the reinforcement and the base matrix, but an effective stir casting process also enhances this interaction.[21] The magnesium alloy composite of AZ31/silicon carbide (SiC)/boron carbide (B_4C) was synthesized via stir casting and evaluated for its machinability and mechanical behaviour. The integration of SiC and B_4C into AZ31 magnesium alloy resulted in high microhardness, improved tensile strength, and reduced elongation behaviour for the combinations of hard ceramic particles, which influence hard machining and tool wear.[22]

Furthermore, the AZ31 alloy hybrid composite was synthesized via stir casting using SiC and graphite particles. The presence of SiC/graphite in the AZ31 alloy matrix is identified as exhibiting maximum tensile and hardness behaviour. However, the presence of hard ceramic particles results in a marginal decrease in elongation behaviour.[23] The AZ91D magnesium alloy hybrid composite, composed of graphite and SiC particles, was produced via stir casting and evaluated for its functional behaviour in accordance with the ASTM standard. The outcome showed that the composite containing 1 wt.% graphite and 5 wt.% SiC exhibited a marginal increase in yield and tensile stress.[24]

Moreover, the fabrication of AZ91 alloy hybrid composites and their properties, as discussed in the context of earlier literature, are presented above. The formation of oxides and the creation of entrapped gas bubbles during the melting and stirring of the magnesium alloy were the major challenges to limiting the overall composite behaviour. The key role of current research is enriching the composite quality with agglomeration and porous free structure, enhancing the particle dispersion, and functional properties like tensile, hardness, and energy absorption behaviour of AZ91 series magnesium alloy hybrid nanocomposite with 0.5 % of a single layer of carbon atom featured graphene filler and 2–6 % of silicon carbide nanoparticles via vacuum-aided stir cast route under argon shield gas, with constant stir speed. The effects of composite processing and the actions of multi-reinforcements on the microstructural, mechanical, and density/porosity behaviour of composites are evaluated and compared with those of the AZ91 cast. Finally, the optimum composite properties are compared with those in earlier literature to highlight the novelty of the current research and the role of hybrid reinforcements in AZ91 alloy.

Materials and Methods

Material and Its Composition Details

Here, the hybrid nanocomposite is designed by the combinations of AZ91 series magnesium alloy as the base matrix of 10 mm length and 20 mm diameter (ingots), and a single layer of carbon atom featured graphene filler (99% purity) and silicon carbide nanoparticles (99.9% purity) is selected as hybrid reinforcements, its size is 0.5 µm length and 30 nm of thickness and 50 nm, respectively. As reported by Kumar et al. [11], graphene is selected at 0.5% due to its wide surface area, which provides better load transfer, increased tensile strength, and leads to grain refinement. According to earlier research [13], nano-SiC is fixed at 2, 4, and 6%, and SiC above 6% shows agglomeration; the composite has higher hardness, which influences the limiting tensile strength.[23] With respect to scanning electron microscope with energy-dispersive X-ray spectroscopy (SEM-EDS) analysis, the composition of AZ91 alloy is confirmed, and its SEM-EDS is presented in Figure 1A–a. Similarly, the SEM-EDS of SiC and graphene is shown in Figure 1b–B and c–C. Table 1 presents the properties of AZ91 series alloy, graphene, and SiC. Both matrix (AZ91) and reinforcements (graphene and SiC) are received from the research and development department, MS. Saveetha University, Chennai, Tamil Nadu, India, which are procured from Coimbatore Metal Mart, Coimbatore, Tamil Nadu, India, and Royal Scientific Supplier, Trichy, Tamil Nadu, India.

Preparation of Composites

In current research, the vacuum-aided stir casting route is preferred to minimize casting defects and enhance composite quality.[15,16] Based on earlier research by Karthik et al. [3] and Krishnakumar et al. [13], the optimized stir cast process parameters for the fabrication of magnesium alloy composites are detailed in Table 2.

A step-by-step flow process for the production of AZ91 alloy, AZ91/0.5% graphene, and AZ91/0.5% graphene/2–6% of nano-SiC composites is presented in Figure 2. According to the composite compositions listed in Table 3, the composites are prepared, and the development procedure for AZ91/0.5% graphene/6% SiC is elaborated. Before the fabrication process, the weights of the base matrix (AZ91) and hybrid reinforcements (graphene/SiC) are measured using a Shimadzu-made AUW220D model anti-vibration digital weighing setup with an accuracy of ±0.01 mg. The moisture content of an ingot-formed AZ91 series alloy was removed through a preheating process (550 °C) conducted in an electrical furnace, with temperature monitored and controlled via a control panel attached to the vacuum-aided stir cast setup. Similarly, the moisture behaviour of graphene and SiC is removed by a

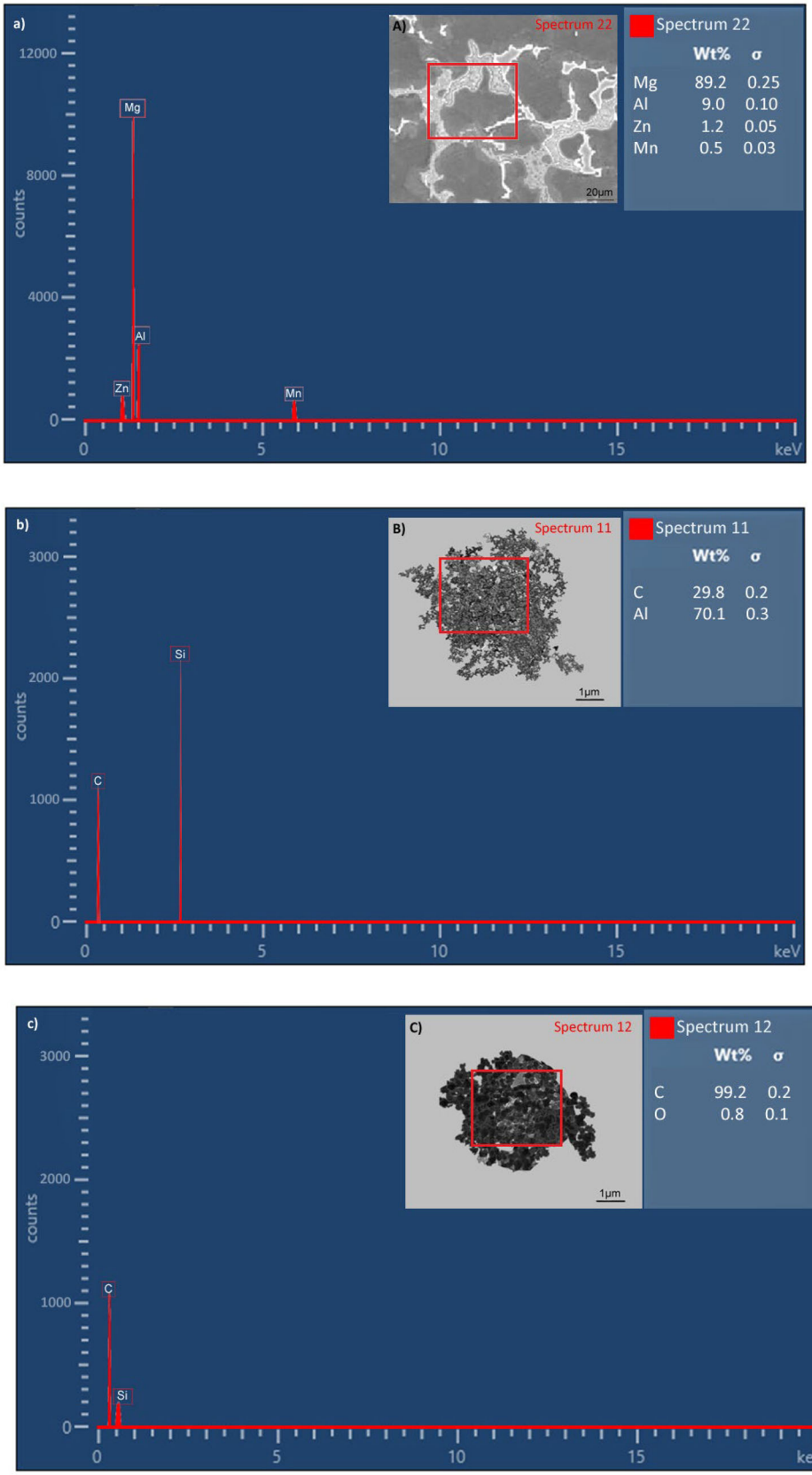

Figure 1. Surface morphology of (B) SEM and (b) EDS of SiC. Surface morphology (SEM-EDS) of A-a) AZ91 alloy, (B–b) SiC and (C–c) Graphene.

Table 1. Properties of Matrix And Reinforcements[3,11]

Materials	Size	Density in g/cm^3	Melting point temperature in °C	Hardness in HV
AZ91	10mm length and 20mm diameter	1.81	595–640	65–80
Graphene	0.5μm length and 30nm of thickness	2.26	3500–3690	1000
SiC	50nm	3.21	2700	2450

Table 2. Optimized Vacuum-Aided Stir Cast Process Parameters[3,13]

Descriptions	Parameters	Values
AZ91 alloy	Preheat temperature	550 °C
	Melting temperature	597–638 °C
	Process temperature	600 °C
Graphene/SiC	Preheat temperature	300 °C
Stir	Temperature	580 °C
	Speed	400 rpm
	Time	10 min
	Feed	0.8 g/cc
	Impeller	1
	Number of blades	2 (stainless steel)
	Blade angle	29 degree
Inert gas/shield gas	Argon	Throughout the process
Die	Preheat temperature	300 °C
	Material	Titanium-coated tool steel
	Dimension	15 cm X 10 cm X 1.5 cm

preheating process (300 °C), which is performed using a muffle furnace. With the control panel, the electrical furnace temperature is increased to 597–638 °C and maintained until the AZ91 alloy melts, as monitored by a PID temperature controller. To limit the oxide formation, the argon shield gas is used throughout the process.[15]

After the process, the temperature of the molten metal is reduced to 600 °C, and the hybrid reinforcement (preheated) is added to it. It helps limit viscosity and air entrapment during stirring.[6] The 400 rpm rated stir speed is maintained for 10 minutes, leading to homogeneous particle dispersion.[13,15] The twin-blade designed stir blade provides better blending behaviour and minimizes cluster formation, resulting in improved bonding strength between the base matrix and reinforcements. The blended composite mixtures are transferred to a 300 °C heated titanium-coated tool steel rectangular die, which leads to minimizing the casting shrinkage and 1X10^5 Pa vacuum pressures are applied, which helps to limit the porosity formation and enhance the quality of composites. Fabricated AZ91 alloy composites are cooled by natural convection to ambient temperature.

Characteristics of Composites

The fabricated composites are examined for their characteristics. Table 4 presents details of the composite characteristics study, including the test instrument make and model, the ASTM standard, test details, and the number of replicates.

The AZ91 alloy composites (15 cm in length, 10 cm in width, and 1.5 cm in thickness) were machined to prepare test samples for surface morphology and mechanical testing. During the preparation of the mechanical test sample, it was extracted along the longitudinal axis of the composite ingot at the midpoint of the plane; surface morphology samples were also extracted.

Results and Discussion

Scanning Electron Microscope with Energy-Dispersive X-Ray Spectroscopy (SEM-EDS)

The rated stir speed, argon shield gas, and vacuum-aided stir casting all contributed to improved composite quality and uniform distribution of graphene and SiC. Here, Figure 1 A–a shows the SEM-EDS-analyzed microstructure of the AZ91 alloy, which clearly reveals the α phase (Mg) and the β phase ($Mg_{17}Al_{12}$). During solidification, secondary phase grains form, thereby limiting the solubility of aluminum [9]. Its grain size is 120±8 μm. Moreover, effective process parameters and applied vacuum pressure resulted in better composite quality, with reduced oxide layers and porosity. With respect to EDS peaks, the presence of the element in the AZ91 alloy is confirmed and highlighted, along with its weight percentage (wt.%) of elements, in the right corner of each EDS peak. This is illustrated in Figure 1A.

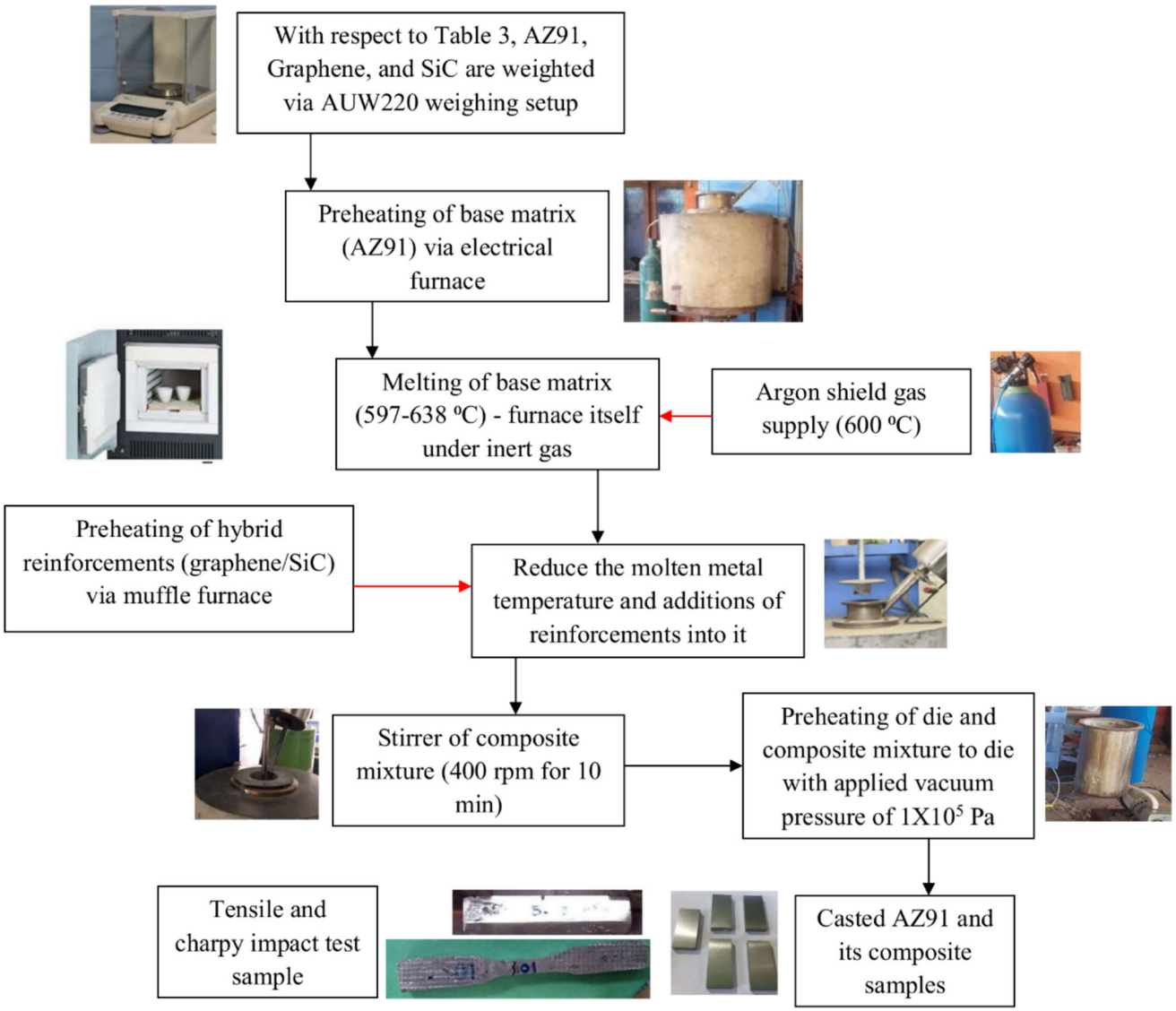

Figure 2. Step-by-step flow process layout for magnesium alloy composite fabrications.

Table 3. Composite Composing Details and Their Weight %

Identification of composites	Weight percentage (wt.%)		
	AZ91	Graphene	SiC
AZ91	100	0	0
AZ91/0.5% Graphene	99.5	0.5	0
AZ91/0.5% Graphene/2% SiC	97.5	0.5	2
AZ91/0.5% Graphene/4% SiC	95.5	0.5	4
AZ91/0.5% Graphene/6% SiC	93.5	0.5	6

Based on the analysis of SEM-EDS, the detailed microstructure analysis of AZ91/0.5% graphene and AZ91/0.5% graphene/2–6% SiC is highlighted in Figure 3A/a—D/d.

Similarly, the microstructure of AZ91 embedded with 0.5% graphene, obtained via vacuum-aided stir casting, is presented in Figure 3b. A high stir speed leads to a wide dispersion of graphene particles. It makes an efficient bonding with the AZ91 matrix, resulting in enhanced stress concentration behaviour and limiting the dislocation of graphene,[11] which leads to higher tensile stress behaviour. The EDS peaks of AZ91/0.5% graphene are shown in Figure 3B. It reached the highest Mg level, and the contributions of other elements, including Al, C, Zn, Mn, and O, are noted. Moreover, the presence of graphene improves nucleation sites, leading to coarse-grain boundaries with an average grain size of 90 ± 6 µm.

Figure 3C/c depicts the SEM-EDS peaks of AZ91/0.5% graphene with 2 % SiC particles, and it is noted that the SiC particles are distributed homogeneously in the AZ91 matrix due to the even stir speed under reduced processing temperature. It helps minimize particle agglomeration and

Table 4. Characteristics Evaluation Details

Test details	Instrument make and mode	Standard	Testing conditions	Dimension	No of replicate	Test significance
SEM-EDS	FESEM-Quattros	ASTM E1508	10 mm distance with high resolution (12 kV power)	10 mm ×10 mm × 10 mm (glassy polished samples)	1	Confirmed with distribution, binding and its elements
Tensile strength	Instron made the 5982 model UTM	ASTME8	5 mm/min cross-head speed	100 mm × 10 mm × 6 mm	3	Yield, tensile, and elongation (5 % allowable error)
Vickers hardness number	Mitutoyo make the HM 210 model Vickers hardness tester	ASTM E92-17	1 kgf load for 10 s dwell time	50 mm × 50 mm × 10 mm	3	Resistance to indentation (5% allowable error)
Charpy impact strength	Zwick made IT30 a model pendulum-type impact tester	ASTM E23	V-notch (150° swing angle) with 40 mm span	55 mm × 10 mm × 10 mm (45° V-notch at 2 mm depth)	3	Energy absorption behaviour (5% allowable error)

shear.[10,13] The combined action of SiC and graphene provided a wide surface contact and better pinning in the base matrix, resulting in enhanced hardness and energy absorption behaviour. Moreover, vacuum pressure helps minimize major casting defects and enriches composite quality by providing a better-interfaced structure. The concentration of SiC is confirmed via EDS (Figure 3C), as the elements of Si and C. Similarly, Figure 3D/d and Figure 3E/e provide the clear microstructure and EDS peaks of AZ91/0.5% graphene/4 and 6 % of SiC composites. It was found that graphene and SiC could occupy a wide surface area, and an increased SiC content leads to more nucleation sites, which strengthen the microstructural bonding, resulting in higher tensile strength behaviour in the composites. Moreover, the variation in graphene and SiC particle size in the AZ91 matrix ensures maximum surface contact and strong adhesion to the base matrix. It increases the mechanical behaviour of composites.[3,17] Furthermore, the composite made with a constant weight percentage of graphene and improved SiC nanoparticle (2, 4, and 6 wt.%) yields more nucleation sites with the Mg17Al12 intermetallic phase, resulting in fine grain boundaries with reduced grain sizes of 68 ± 5, 50 ± 6, and 35 ± 2 μm, respectively. However, optimized vacuum-aided stir casting parameters and variations in particle size improved composite quality, enhancing hybrid surface contact and resulting in higher functional behaviour.

Physical Characteristics

According to the investigation, density plays a major role in determining the composite's weight and its actual/calculated density behaviour, as shown in Figure 4. Based on Archimede's principle and the rule of mixture, the actual and calculated densities were measured. Using Eqn. 1,[3,13] the composite's porosity was then calculated.

$$\text{Porosity}\% = \frac{(\text{calculated} - \text{actual})\text{density}}{\text{calculated density}} \times 100 \qquad \text{Eqn. 1}$$

Here, Figure 4 represents the density of actual and calculated porosity percentages for AZ91, AZ91/0.5% graphene, and AZ91/0.5% graphene/2–6% SiC composites. Due to unavoidable porosity, the actual density is lower than the calculated density. The measured density behaviour of AZ91, AZ91/0.5% graphene, and AZ91/0.5% graphene with 2, 4, and 6% SiC is 1.79, 1.80, 1.82, 1.85, and 1.88 g/cm^3, respectively.

The incorporation of SiC and graphene into the AZ91 matrix is responsible for the increase in density and obeys the rule of mixtures. An optimized stir casting process, along with an improved content of nano-SiC and 0.5% graphene, resulted in a significant enhancement in density behaviour. Additionally, the porosity of the magnesium alloy without reinforcement decreased from 1.05% to 0.70% when compared to composites with 0.5% graphene and 2-6% SiC particles. The varying sizes of graphene and SiC particles can fill voids and enhance bonding quality, leading to finer grain boundaries and reduced porosity in the composite.[5]. Furthermore, the increased content of nano-SiC leads to a greater number of nucleation sites during solidification, refining the structure and reducing porosity.[7] Furthermore, a higher content of nano-hybrid reinforcements within the magnesium matrix improved surface contact. The application of vacuum pressure also minimized porosity, resulting in enhanced bonding strength.[1]

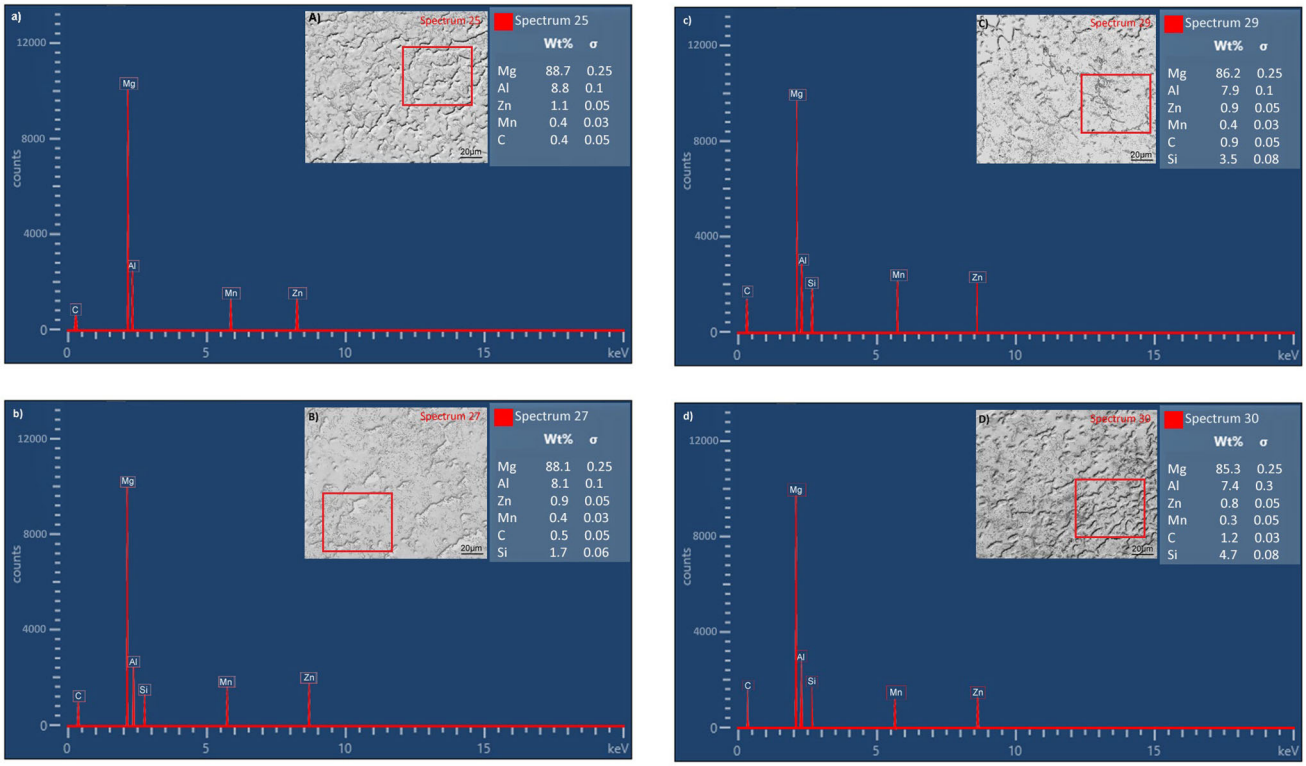

Figure 3. SEM-EDS microstructure of (A–a) AZ91/0.5% graphene, (B–b) AZ91/0.5% graphene/2% SiC, (C–c) AZ91/ 0.5% graphene/4% SiC, and (D–d) AZ91/0.5% graphene/6% SiC.

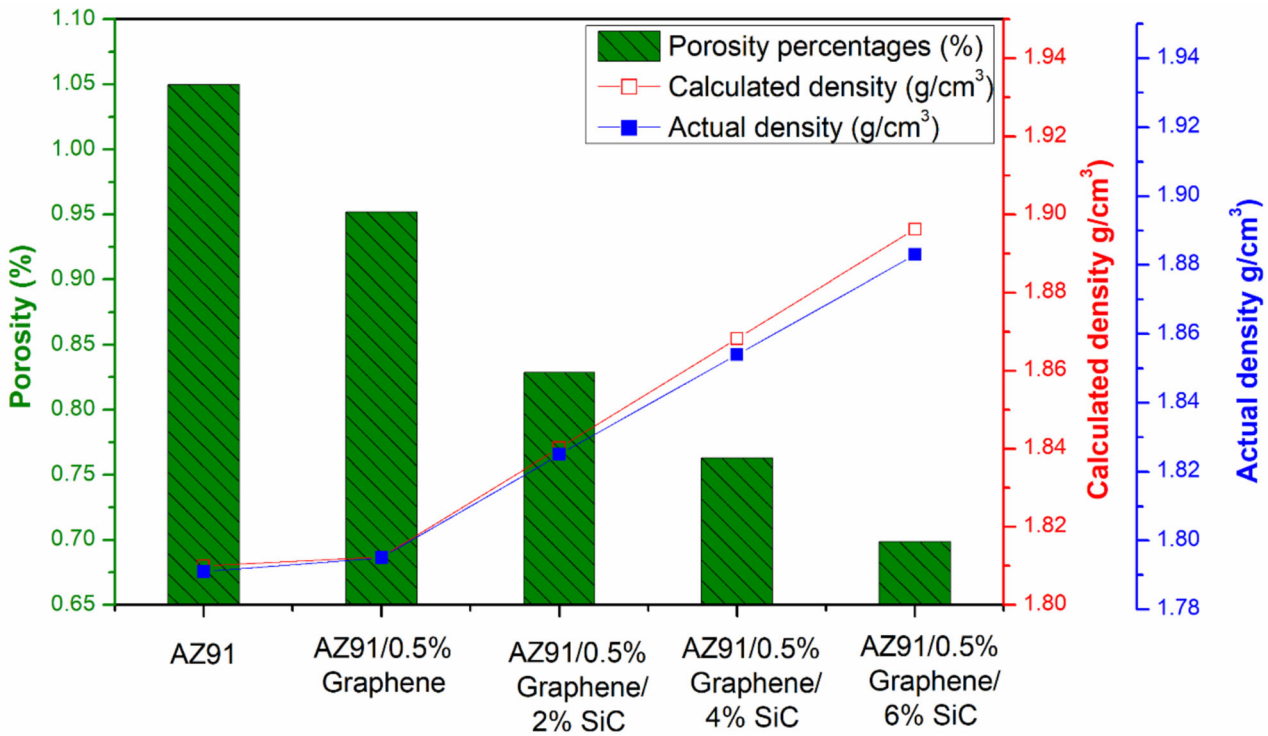

Figure 4. Density (actual/theoretical)/ porosity percentage of developed samples.

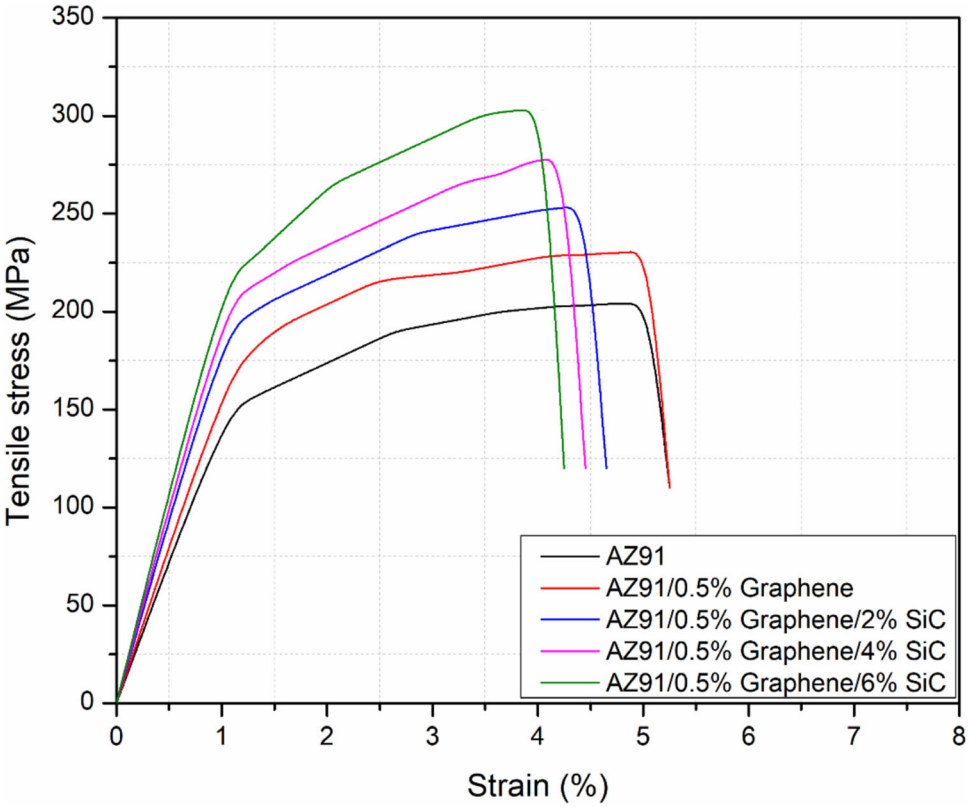

Figure 5. AZ91 alloy, AZ91 alloy/0.5% graphene, and AZ91/0.5% graphene/2-6% of SiC composite's stress–strain curve.

Table 5. Average Values of Yield and Tensile Strength, Elongation % and Elastic Modulus Behaviour of Composites

Identification of composites	Yield strength (YS) MPa	Error in YS	Tensile strength (UTS) MPa	Error in UTS	Elongation (%) %	Error in Elongation	Young's modulus (E) GPa	Error in E
AZ91	165	6.60	205	10.25	5.4	0.216	43	1.5
AZ91/0.5% Graphene	188	7.52	232	6.96	5.2	0.26	48	2.5
AZ91/0.5% Graphene/2% SiC	198	7.92	254	10.16	4.7	0.188	52	2
AZ91/0.5% Graphene/4% SiC	212	10.60	278	13.9	4.4	0.22	58	1
AZ91/0.5% Graphene/6% SiC	236	11.80	303	12.12	4.2	0.168	61	3

Tensile Stress–Strain Performance

Stress–strain performance of AZ91, AZ91/0.5% graphene, and AZ91/0.5% graphene/2-6% of SiC composites are presented in Figure 5. Table 5 indicates the average values of yield, tensile strength, elongation %, and elastic modulus behaviour of the tested composite samples.

It is observed from Figure 5 that the combined actions of graphene and SiC nanoparticles in AZ91 alloy result in an optimum tensile stress behaviour, which is greater than that of the AZ91 series alloy. The rated stir speed and applied vacuum pressure significantly influenced the dispersion of wide graphene and SiC particles, and an effective interface led to a higher load-carrying capacity, resulting in an enhanced tensile stress behaviour. The wide graphene/SiC particle dispersion in the AZ91 matrix is shown in Figure 3b–d.

Here, the tensile stress–strain behaviour of AZ91 cast is found to be 205 MPa and 5.4%, respectively, which is nearly identical to the actual tensile stress–strain behaviour.[25] While the AZ91 alloy embedded with 0.5% graphene exhibits a tensile stress of 232 MPa and a strain of 5.2%, it shows tensile stress–strain behaviour. The presence of 0.5% graphene in AZ91 alloy improves stress concentration behaviour and enhances interfacial adhesion with the base matrix, thereby limiting the displacement of reinforcement particles under higher tensile loads.[10] This is the reason for the enrichment of tensile stress behaviour. Moreover, the contribution of graphene enables it to endure the maximum load and may influence brittle failure, resulting in reduced elongation behaviour, as shown in Figure 5. Moreover, the tensile stress performance of the AZ91/0.5% graphene/SiC composite is significantly improved, from 254 to 303 MPa, with an increase in SiC content from 2% to 6%. The highest tensile stress of 303 MPa is observed in the AZ91/0.5% graphene/6% SiC composite. The increased content of SiC particles in AZ91/0.5% graphene composite exposed more nucleation sites due to the rated stir speed and applied vacuum pressure. The resulting fine grain boundaries facilitate efficient bonding between the base matrix and reinforcement,[9,13] withstand the maximum stress concentration, and lead to superior tensile stress behaviour.

However, the improved contribution of SiC particles in AZ91 alloy/0.5% graphene led to reduced ductility, resulting in a marginal reduction in strain percentage.[13] The AZ91/0.5% graphene/2-6% SiC composite exhibits strains of 4.7%, 4.4%, and 4.2%. However, the tensile stress behaviour of AZ91/0.5% graphene/6% SiC composite is noted to be 47.8%, 10%, and 73% better than the AZ91 cast alloy without graphene and SiC, AZ91/10% fly ash [3], and Al-Zn-Mg with 6% Si_3N_4/95 BN composites.[14] According to the investigation of tensile stress behaviour of composites, the fracture surface of AZ91 alloy, AZ91 alloy /0,5 % graphene, and AZ91/0.5 % graphene and 2–6 % of SiC is shown in Figure 6a–e.

Here, Figure 6a presents the tensile fracture surface of AZ91 alloy and ductile fracture is noted due to the presence of soft magnesium without filler material has plastic deformation. The composite containing 0.5 wt.% graphene exhibited localized failure. However, the presence of graphene particles improves stress concentration behaviour and minimizes plasticity. Furthermore, the combination of SiC and graphene exhibits better stress concentration behaviour, and an increasing content of SiC leads to a greater number of nucleation sites, thereby strengthening the bonding, which results in high stress concentration cleavage planes being observed. Based on the tensile stress–strain performance, the AZ91/0.5% graphene/6% SiC hybrid composite exhibited the optimal stress behaviour (303 MPa), which was higher than that of the other composite samples.

Regarding the optimum tensile stress behaviour, the AZ91/0.5% graphene/6% SiC hybrid composite undergoes tensile fracture analysis via SEM-EDS, and its microstructure is presented in Figure 6e–f. The elongated failure mechanism is noted in Figure 6, and the elongated dimples are highlighted. The presence of SiC particles in the AZ91 matrix acts as a better barrier, limiting the crack propagation and enduring the maximum stress concentration behaviour. However, most of the short dimples seen in Figure 6 could endure the maximum load and failure at their contact point due to the improved content of SiC. They may act as brittle, resulting in reduced elongation behaviour of the composite. It is represented in Figure 5. However, the combined action of graphene and SiC with varying particle sizes could fill the void gap and strengthen the interface, resulting in superior tensile stress behaviour.[13] The contribution and microstructural images of AZ91/0.5% graphene/6% SiC are provided in Figure 3D.

Vickers Hardness Number

According to the references in Figure 7, the Vickers hardness results for AZ91, AZ91/0.5% graphene, and AZ91/0.5% graphene/2–6% SiC composites are presented with error bars.

The combined action of graphene and SiC particles in the AZ91 matrix improved the composite's indentation resistance. The improved SiC nanoparticle content in the AZ91/0.5% graphene composite was reflected in a significant increase in Vickers hardness, exceeding that of the other samples. The varied particle sizes of graphene and SiC could fill the void gap and provide strong bonding with the matrix, thereby improving resistance to the applied load.[9,10] This mechanism is responsible for the optimal enhancement in the Vickers hardness value of the composites. Moreover, the AZ91 cast alloy without graphene and SiC particles measured a Vickers hardness value of 72 HV, and when embedded with 0.5% graphene, it increased to 75 HV. It shows the upward trend in Vickers hardness values (85 HV) due to graphene efficiently pinning the AZ91 matrix, limiting the applied load and enhancing resistance to scratching.[11]

At the same time, the AZ91/0.5% graphene with 2, 4, and 6% SiC content exhibited significant increases in hardness values, reaching 92, 98, and 105 HV, respectively. The combination of 30 nm graphene and 50 nm SiC particles, treated with constant stirring under an argon shield gas, provided more nucleation sites, resulting in a reduced particle gap and a stronger pinning mechanism, thereby increasing the hardness of SiC-embedded AZ91/0.5% graphene composites. Furthermore, the AZ91/0.5% graphene with 6% SiC has found an optimum value, which is 46%, 10%, and 21% greater than the AZ91 alloy without

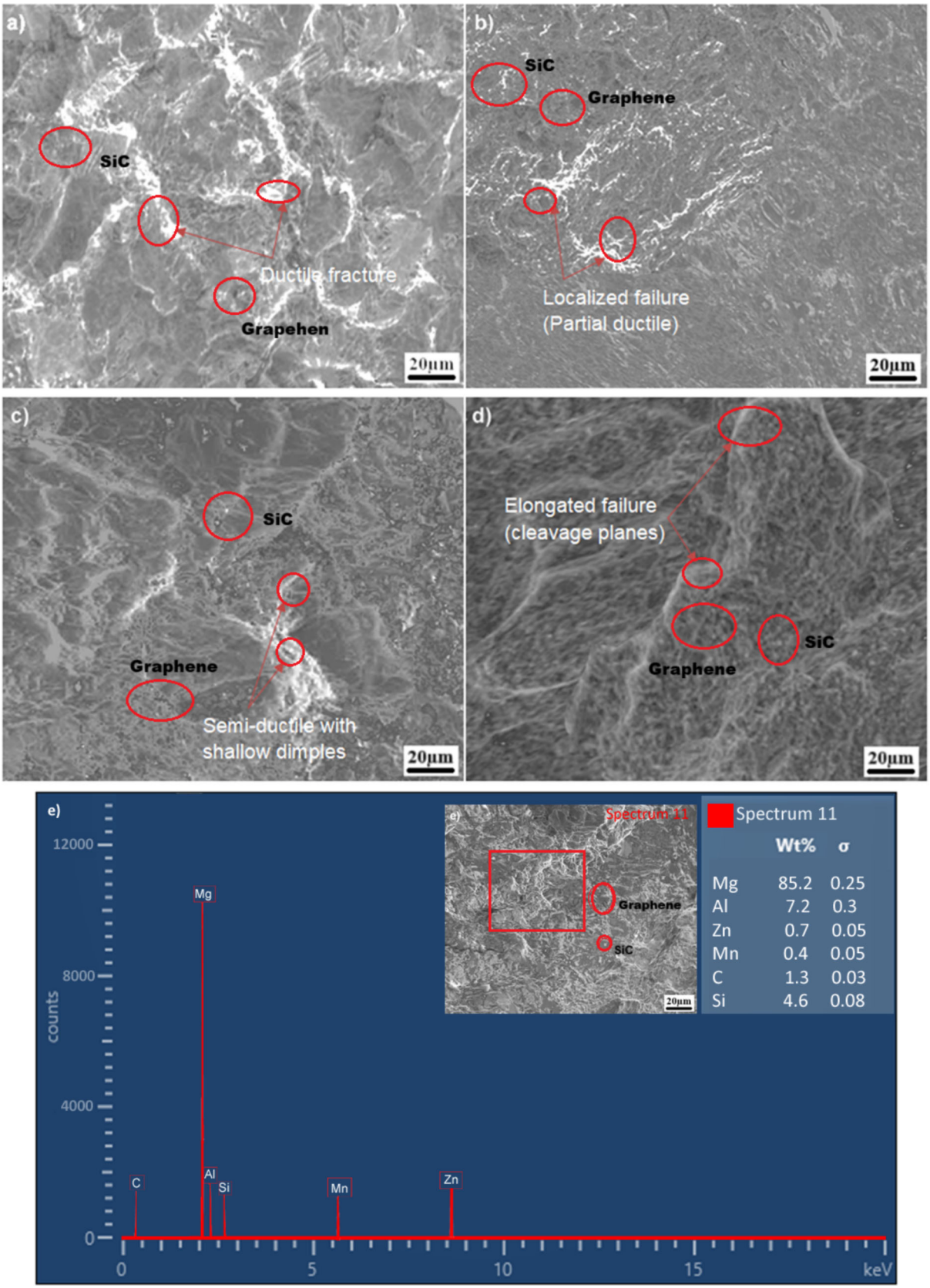

Figure 6. Tensile fracture surface morphology of (a) AZ alloy, (b) AZ91/0.5% graphene, (c) AZ91/0.5% graphene/2% SiC, (d) AZ91/0.5% graphene/4% SiC, and (e) SEM-EDS image of AZ91/0.5% graphene/6% SiC.

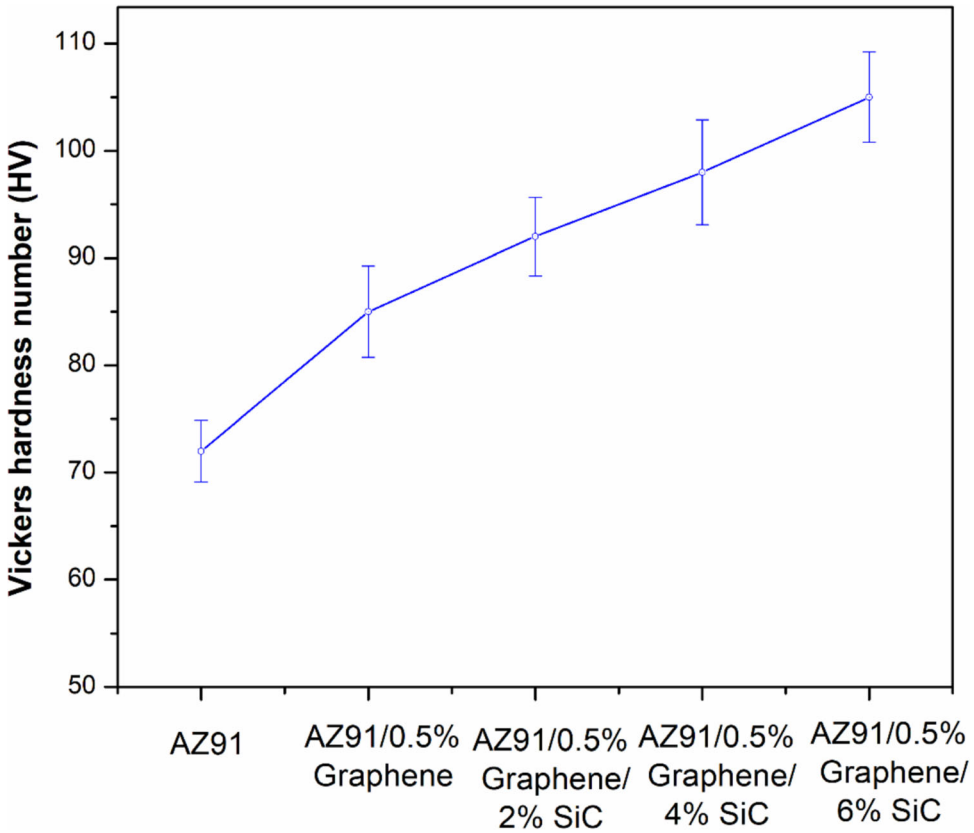

Figure 7. AZ91 alloy, AZ91 alloy/0.5% graphene, and AZ91/0.5% graphene/2-6% of SiC composite's Vickers hardness number.

graphene/SiC, AZ91/10wt.% fly ash [3], and AZ91/35 BN/5% TiB_2 composites.[7]

Charpy Impact Toughness

The energy absorption performance (Charpy impact toughness) for AZ91, AZ91/0.5% graphene, and AZ91/0.5% graphene/2-6% SiC composites, with their average values, is presented in Figure 8. Better graphene/SiC pinning in an AZ91 matrix results in higher energy absorption than in monolithic and 0.5% graphene-embedded composite samples. The selection of particle size and process parameters improves the composite's microstructural quality. It shows the efficient interface-bonded surface result, ensuring the maximum energy absorption behaviour.[7] Here, the Charpy impact strength (energy absorption) behaviour of AZ91 alloy without hybrid reinforcement is found to be 11.6 J/mm^2, and the base matrix of the AZ91 series alloy, incorporated with 0.5% graphene, exhibits a marginal increase in energy absorption behaviour (12.1 J/mm^2). The graphene particle exhibits better intrinsic behaviour and an efficient pinning mechanism, which explains its enhanced energy absorption. Furthermore, incorporation of 50 nm SiC into the AZ91/0.5% graphene composite is noted to progressively enhance energy absorption behaviour, with 12.6, 13.2, and 13.7 J/mm2 observed for 2, 4, and 6 % SiC in the AZ91/0.5% graphene composite.

The increased SiC content at the rated stir speed resulted in a homogeneous particle distribution. It strengthened the AZ91 structure with improved SiC surface contact (Figure 3D), promoting the structure through fine grain boundaries, resulting in improved energy absorption behaviour. However, the AZ91/0.5% graphene/6% SiC hybrid composite exhibited optimal energy absorption behaviour and 18% better performance than the AZ91 alloy fabricated without reinforcements.

Regarding the energy absorption behaviour, the AZ91/0.5% graphene/6% SiC composite exhibits enhanced energy absorption, as shown in its fracture surface in Figure 9A–a. The combined action of graphene/SiC and optimized stir cast process parameters yielded a balanced energy absorption behaviour with enhanced load transfer, resulting in higher energy absorption. With EDS mapping, it clearly indicates that the SiC and graphene particles contribute to an efficient bond with the base matrix, with clear peaks of Si and C highlighted in Figure 9A–a. Efficient bonding of graphene and SiC to AZ91 delays crack propagation and maximizes energy absorption.[11,12] However, the contribution of SiC leads to a fine grain structure with improved interfaces, providing higher toughening in

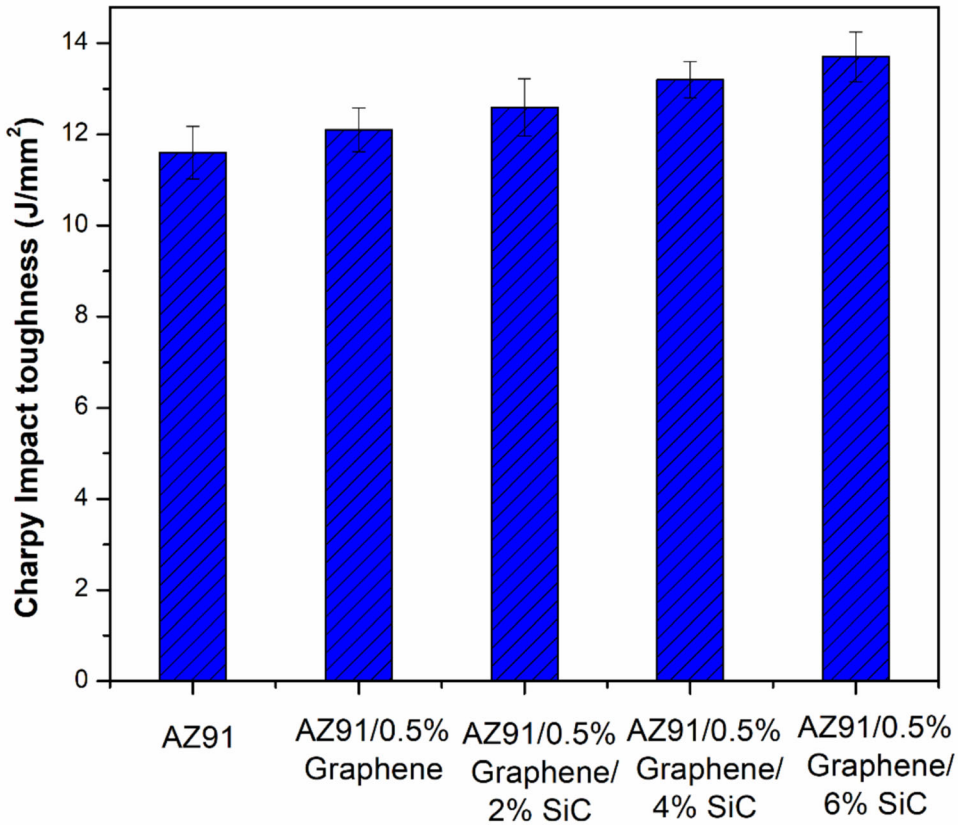

Figure 8. AZ91 alloy, AZ91 alloy/0.5% graphene, and AZ91/0.5% graphene/2-6% of SiC composite's Charpy impact toughness.

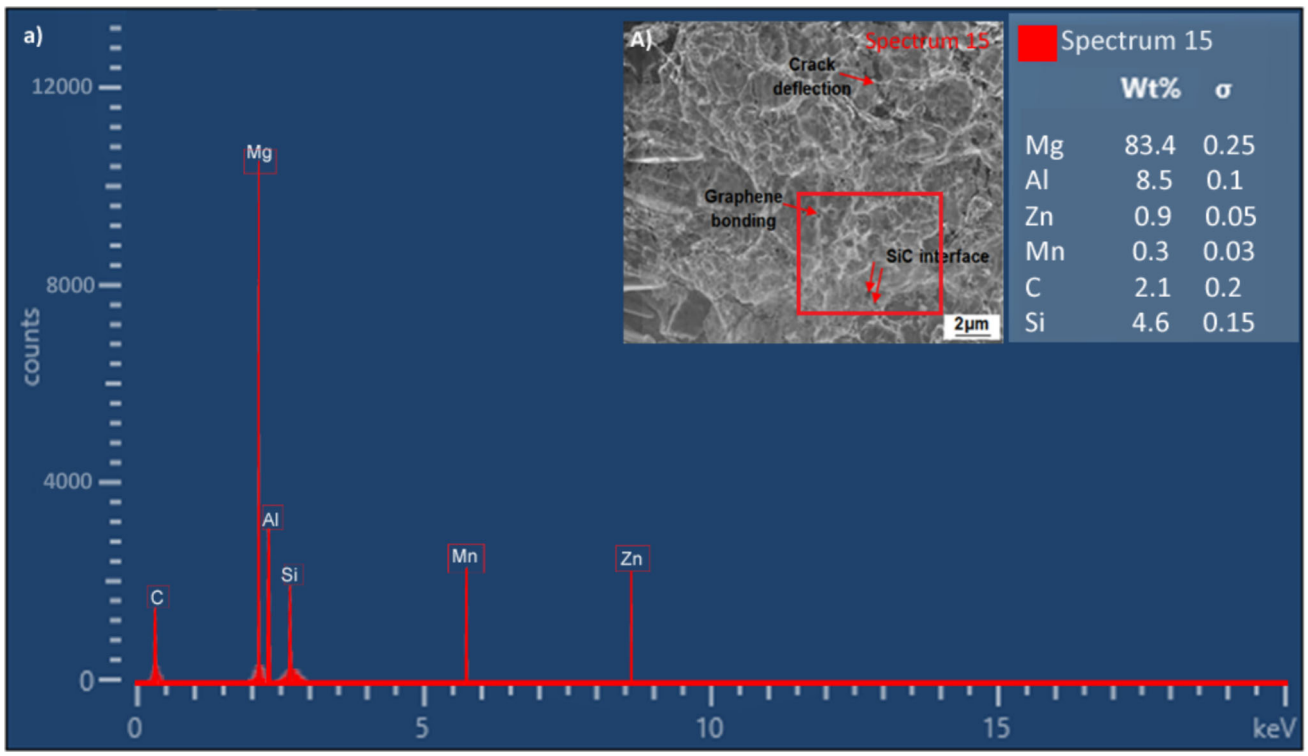

Figure 9. Microstructure of impact fracture surface (SEM-EDS)—AZ91/0.5% graphene/6% SiC composite.

Table 6. AZ91/0.5% Graphene/6% Sic Hybrid Composite Behaviour Related to Earlier Research

Composite details	Fabrication details	Density g/cm^3	Porosity %	Grain size μm	Tensile strength MPa	Hardness HV	Energy absorption J/mm^2	Reference
AZ91/0.5% Graphene/6% SiC	Vacuum-aided stir cast	1.883	0.7	35	303	105	13.7	Current research
AZ91/3% BN/ 5% TiO_2	Two-step stir cast	1.917	0.78	43	247	87	17.1	7
AZ91/1.5% Al_2O_3/5 % TiB_2	Ultrasonic-aided stir cast	–	–	–	185	171	1.36	12
Al-Zn-Mg with 6% Si_3N_4/ 9% BN	Vacuum-aided stir cast	–	0.82	–	175	145	3.1	14
AZ31/5 % SiC/ 5 % Graphite	Bottom type stir casting	1.85	2	41	265	98	–	23
AZ91D/ 5 wt.% SiC/ 1 wt.% Graphite	Stir cast	1.89	–	–	171	–	–	24

the composite and influencing its superior impact strength. The crack deflection, SiC, and graphene interface bonding, which limits crack propagation, are highlighted in Figure 9A.

Regarding investigation outcomes, the AZ91/0.5% graphene/6% SiC hybrid composite exhibited optimal functional behaviour and improved microstructural quality. For highlighting the novelty of the present research on AZ91/0.5% graphene/6% SiC hybrid composite, related to past literature, as presented in Table 6.

The combination of 0.5% graphene and 6% SiC in the AZ91 matrix resulted in lower density and porosity. Its density is 2% higher than that of the AZ91/3% BN/5 % TiO_2 hybrid composite.[7] Likewise, the porosity percentage is reduced by 11% and 17% compared to the two-step stir cast developed AZ91/3% BN/5 % TiO_2 hybrid composite [7] and the vacuum-aided developed Al-Zn-Mg with 6% Si_3N_4/9% BN hybrid composites.[14] Combined actions of SiC and graphene in AZ91 matrix hybrid composite tensile strength is enriched by 22.6%, 63%, 73%, 14.3% and 77% better than the two-step stir caste fabricated AZ91/3% BN/ 5% TiO_2,[7] Ultrasonic-aided stir cast prepared AZ91/1.5% Al_2O_3/5 % TiB_2,[12] vacuum-aided stir cast Al-Zn-Mg with 6% Si_3N_4/9% BN composites,[14] the AZ31/5 % SiC/ 5 % Graphite synthesized via bottom pouring stir cast,[23] and stir cast made AZ91D/ 5 wt.% SiC/ 1 wt.% Graphite.[24] Similarly, the Vickers hardness value of the AZ91/0.5% graphene/6% SiC hybrid composite is 21% and 7% better than that of the two-step stir cast fabricated AZ91/3% BN/5% TiO_2[7] and AZ31/5% SiC/5 % Graphite.[23] The additions of SiC content into AZ91/0.5% composite found a progressive hike in energy absorption behaviour, and 341% better than the vacuum-aided stir cast Al-Zn-Mg with 6% Si_3N_4/ 9% BN composites.[14]

Conclusion

The magnesium alloy series of AZ91 hybrid composites was composed of 0.5% graphene and 2–6% nano-silicon carbide (SiC) particles via a vacuum-aided stir cast route, which was maintained by a rated stir speed and argon shield gas used throughout the process. The effect of vacuum-aided stir processing and hybrid (graphene and SiC) on surface morphological, mechanical and density/porosity behaviour of hybrid composites was investigated, and its outcomes were compared with AZ91 and AZ91/0.5% graphene composites. Based on the investigation outcomes, the AZ91/0.5% graphene/6% SiC composite exhibited the best functional behaviour among the composites. Important key findings are concluded below.

- With optimized vacuum stir cast process parameters and a range of graphene and SiC sizes, a homogeneous graphene and SiC dispersion with improved composite quality was confirmed via scanning electron microscopy with energy-dispersive X-ray spectroscopy (SEM-EDS) analysis. The role of vacuum pressure was found to improve bonding quality and minimize casting defects.
- The tensile stress, Vickers hardness, and energy absorption behaviour of the AZ91/0.5% graphene/6% SiC hybrid composite were identified as having maximum values, which were 48%, 46%, and 18% higher than those of AZ91 without graphene or SiC particles.

- Furthermore, the actual density of the AZ91/0.5% graphene/6% SiC hybrid composite is noted as 1.883 g/cm^3, with a reduced porosity of 0.7%.
- With its improved density and enhanced mechanical behaviour, the AZ91/0.5% graphene/6% SiC hybrid composite offers potential for automotive structural frame applications and for further research into dry sling wear performance under varied loads, sliding speeds, and distances, as well as for the composite's recycling with consideration for environmental aspects.

Author Contributions

All authors contributed to the conception and design of the study. Material preparation, data collection, and analysis were performed by Ramesh Dnyando Sul, Nitin Kundlik, Aman Sharma, V. Muthuraman, Sendil kumar, Nagabhooshanam Nagarajan, BEVL Naidu, Ramya Maranan, and T. Thirugnanasambandham. The first draft of the manuscript was written by [T. Thirugnanasambandham] and all authors provided language help, writing assistance, and proofreading of the manuscript. All authors read and approved the final manuscript.

Funding

The authors did not receive support from any organization for the work submitted. No funding was received to assist with the preparation of this manuscript. No funding was received for conducting this study. No funds, grants, or other support were received.

Data Availability

All the data required are available within the manuscript

Conflict of interest The authors have no relevant financial or non-financial interests to disclose. The authors have no competing interests to declare relevant to this article's content. All authors certify that they have no affiliations with or involvement in any organization or entity with any financial or non-financial interest in the subject matter or materials discussed in this manuscript. The authors have no financial or proprietary interests in any material discussed in this article.

Ethical approval This is an observational study. Enrichment of surface morphology and mechanical behaviour of magnesium alloy composite made with hybrid reinforcements via vacuum aided stir cast process, the Research Ethics Committee has confirmed that no ethical approval is required.

Informed consent Informed consent was obtained from all individual authors included in the study.

REFERENCES

1. Y. Yang, X. Xiong, J. Chen, X. Peng, D. Chen, F. Pan, Research advances in magnesium and magnesium alloys worldwide in 2020. J. Magnes. Alloy. (2021). https://doi.org/10.1016/j.jma.2021.04.001
2. B. Chandra Kandpal, N. Johri, L. Kumar, A. Tyagi, V. Joshi, U. Gupta, Stir casting technology for magnesium-based metal matrix composites for bio-implants—a review. Mater. Today Proc. **62**, 4519–4525 (2022). https://doi.org/10.1016/j.matpr.2022.04.957
3. R. Karthik, N. Shiva Sankaran, K. Venkatesh Raja, R. Venkatesh, Characteristics performance evaluation of AZ91-fly ash composite developed by vacuum associated stir processing. Int. J. Cast Met. Res. **37**(4–6), 257–264 (2024). https://doi.org/10.1080/13640461.2024.2364129
4. Kumar, D., Phanden, R. K., Thakur, L. (2020). A review on environment friendly and lightweight magnesium-based metal matrix composites and alloys. In: *Materials Today: Proceedings* 38 359–364). Elsevier Ltd. https://doi.org/10.1016/j.matpr.2020.07.424
5. T Thirugnanasambandham J Chandradass R Venkatesh P Sharma MME Soudagar S. Almoallim, H., Al Obaid, S. 2024 Silicon carbide-embedded AZ91E alloy nanocomposite hybridized with chopped basalt fibre: performance measures. International Journal of Cast Metals Research. 37 4–6 265 275 https://doi.org/10.1080/13640461.2024.2395124
6. P. Monish, K.L. Hari Krishna, K. Rajkumar, *Manufacturing and characterization of magnesium composites reinforced by nanoparticles: a review* (Taylor and Francis Ltd., Materials Science and Technology (United Kingdom), 2023). https://doi.org/10.1080/02670836.2023.2194745
7. A. Sharma, K. Karthik, R. Kumar, P.K.K. Vicekananda, M. Vinayagam, M.E.M. Soudagar, S.A. Obaid, S.A. Alharbi, Hybrid reinforcement actions on microstructural physical and mechanical properties of magnesium alloy composite by two-step stir casting process. Inter. Metalcast. (2025). https://doi.org/10.1007/s40962-024-01537-9
8. K.N. Braszczyńska-Malik, Microstructure and mechanical properties of hybrid AZ91 magnesium matrix composite with Ti and SiC particles. Materi. (2022). https://doi.org/10.3390/ma15186301
9. P. Gollapalli, M. Pant, A.R. Chandra, M.K. Surappa, On the microstructural mechanical damping wear properties of magnesium alloy AZ91-3 vol% SiCP-3 vol% fly ash hybrid composite and property correlation thereof. J. magnesium alloys (2025). https://doi.org/10.1016/j.jma.2025.03.016
10. S. Thanikodi, Effect of graphene nanoparticle reinforcement on the mechanical properties of ZE41/graphene nanocomposites prepared by stir casting route. Int. J. Adv. Manuf. Technol. **136**, 15–25 (2025). https://doi.org/10.1007/s00170-024-13508-9

11. N.S. Kumar, G.G. Sozhamannan, Investigating the effect of mechanical properties of magnesium alloy (AZ91D) reinforced with graphene metal matrix composite by stir casting method. Mater. Today Proc. **64**, 95–100 (2022). https://doi.org/10.1016/j.matpr.2022.03.718
12. D. Kumar, L. Thakur, Influence of hybrid reinforcements on the mechanical properties and morphology of AZ91 magnesium alloy composites synthesized by ultrasonic-assisted stir casting. Mater. Today Commun. (2023). https://doi.org/10.1016/j.mtcomm.2023.105937
13. S. Krishnakumar, M. Ali, R. Prakash, Fabrication of nano SiC and BF-bonded magnesium alloy (AZ80) hybrid nanocomposite via liquid state stir casting process: characteristics study. Int. J. Cast Met. Res. **37**(3), 196–207 (2024). https://doi.org/10.1080/13640461.2024.2355615
14. L. Tharanikumar, B. Mohan, G. Anbuchezhiyan, Enhancing the microstructure and mechanical properties of Si3N4-BN strengthened Al-Zn-Mg alloy hybrid nanocomposites using vacuum assisted stir casting method. J. Mater. Res. Technol. **20**, 3646–3655 (2022). https://doi.org/10.1016/j.jmrt.2022.08.093
15. Anand, N., Ramachandran, K. K., & Bijulal, D. (2019). Microstructural, mechanical and tribological characterization of vacuum stir cast Mg-4Zn/Si3N4-magnesium matrix nanocomposite. In: *Materials Today: proceedings* (Vol. 46, pp. 9387–9391). Elsevier Ltd. https://doi.org/10.1016/j.matpr.2020.03.053
16. H.I. Kurt, E. Ergul, A.B. Basyigit, M. Oduncuoglu, N.F. Yilmaz, Development and characterization of Al2024/magnesium oxide/CNTs/ hybrid composites via stir casting method. Proc. Inst. Mech. Eng. Part E J. Process Mech. Eng. **237**(5), 1854–1865 (2023). https://doi.org/10.1177/09544089221128368
17. T. Thirugnanasambandham, J. Chandradass, Fabrication and characteristization of bagasse ash particle (BAP) reinforced magnesium (AZ91E) alloy composite by vacuum stir casting. IOP Conference Series: Mater. Sci. Eng. (2020). https://doi.org/10.1088/1757-899X/993/1/012133
18. P. Kaliyannan, M. Perumal, J. Manivannan, Enhancing mechanical and functional properties of LM25 alloy through squeeze cast hybrid nanocomposite incorporating breadfruit seed husk ash and graphite nanoparticles. Int. J. Cast Met. Res. **37**(1), 12–21 (2023). https://doi.org/10.1080/13640461.2023.2285176
19. Das, A.D., Kamatchi, R.M., Kaliyaperumal, G., Ajin, M. and Shanmugam, R., (2024). Synthesis and functional behavior of sisal fiber-incorporated epoxy hybrid nanocomposite enriched by nano-SiC. *Journal of The Institution of Engineers (India): series D*. https://doi.org/10.1007/s40033-024-00683-y
20. De Poures, M.V, Sudhir Chakravarthy, K., Jabihulla Shariff, M. D., Srinivasa Reddy, Y., Siva Prasad, V., Sreenivasa Rao, K., Kaliyaperumal, G., Kishore Kumar, V. (2024). Excellence of nano SiC on mechanical behaviour of low density polyethylene hybrid nanocomposite. Journal of the Institution of Engineers (India) Series D. https://doi.org/10.1007/s40033-024-00713-9
21. D. Jayaprakash, K. Niranjan, B. Vinod, Studies on mechanical and microstructural properties of aluminium hybrid composites: influence of SiC/gr particles by double stir-casting approach. SILICON **15**(3), 1247–1261 (2023). https://doi.org/10.1007/s12633-022-02106-7
22. A.G. Mohan Das Gandhi, P.M. Gopal, R. Shenbagaraj, V. Kavimani, Effect of SiC reinforcement on mechanical and machinability characteristics of mg/SiC/B4C hybrid composite developed through stir casting. SILICON **15**(13), 5635–5645 (2023). https://doi.org/10.1007/s12633-023-02444-0
23. I. Veeranjaneyulu, V. Chittaranjan Das, S. Karumuri, Investigation of mechanical properties and microstructure of AZ31-SiC-graphite hybrid nanocomposites fabricated by bottom pouring-type stir casting machines. Adv. Mater. Sci. Eng. **2023**, 1–8 (2023). https://doi.org/10.1155/2023/3402348
24. A.P.A. Amalan, N.M. Sivaram, An anisotropy study on microstructure and tensile strength of silicon carbide and graphite particle reinforced AZ91D hybrid composite. Int. J. Mater. Eng. Innov. **14**(2), 136 (2023). https://doi.org/10.1504/ijmatei.2023.130130
25. SivaChandran, S., Maridurai, T., Baskar, S., Sivashankar, N. and Arivazhagan, R. (2022). Magnesium alloy machining and its methodology: a systematic review and analyses. In: AIP Conference Proceedings, 2473, (1). AIP Publishing. https://doi.org/10.1063/5.0096398